Plasmonic coupling on dielectric nanowire core–metal sheath composites

2010 Nanotechnology 21 085705

(http://iopscience.iop.org/0957-4484/21/8/085705)

Nanotechnology **21** (2010) 085705 (5pp) doi:10.1088/0957-4484/21/8/085705

Plasmonic coupling on dielectric nanowire core–metal sheath composites

Hua Qi, Dimitri Alexson, Orest Glembocki and S M Prokes

Electronics Science and Technology Division, Naval Research Laboratory, Washington, DC 20375, USA

E-mail: huaqi@ccs.nrl.navy.mil and Prokes@estd.nrl.navy.mil

Received 16 October 2009, in final form 5 January 2010
Published 25 January 2010
Online at stacks.iop.org/Nano/21/085705

Abstract

We have developed dielectric core/metal sheath nanowire (NW) composites for surface-enhanced Raman scattering (SERS), in which an electroless (EL) Ag plating approach was employed. The NW surface was uniformly covered with a high density of 3D silver islands, having a diameter in the 20–30 nm range and spaced less than ≈10 nm apart. In comparison with the silver deposition via e-beam evaporation, the EL coating approach has the advantage of full metal coverage of the NWs. This approach also provides a fast and simple way to completely cover any nanostructures with Ag, including nanowires, regardless of the orientation or shape. SERS measurements were performed using benzene thiol and the SERS signal strength of the EL-coated NW composites was significantly greater than expected, since the surface plasmon resonance (SPR) of 20 nm Ag nanospheres is weak and in the UV, while our measurements were performed using a 514.5 nm laser line. However, we have modeled this system using our electric field calculations and the results indicate that the strong SERS signal is due to plasmonic coupling of neighboring closely spaced islands, as well as an enhanced substrate effect. In addition, the nanowire core serves as a template for the formation of these small, closely spaced Ag islands, resulting in the strong SERS signal.

(Some figures in this article are in colour only in the electronic version)

1. Introduction

There has been significant interest in the design of a variety of nanostructures for surface-enhanced Raman spectroscopy (SERS) sensing applications [1–6]. SERS is a sensitive technique that results in the enhancement of Raman scattering from molecules adsorbed on metallic nanostructured surfaces. Theoretically, the enhancement factor can be as high as 10^{12}, which would allow this technique to be sensitive enough to detect single molecules [7–11]. Varieties of SERS architectures have been developed including roughened metal surfaces [12], colloids [13], island films [14], self-assembled nanoparticles [15] and arrays of nanoellipsoids [16]. Recently, nanowires (NWs) have been shown to be effective for SERS sensing due to their unique geometry, which is favorable for the formation of the SERS hot spots [17, 18]. Core/metal sheath nanowire composites show additional advantages, such as highly sensitive SERS signals and a shift of the surface plasmon resonance (SPR) into the near-IR, which is a requirement for eye safety. In our previous work [17], the silver and gold metal films on the nanowires were formed via a line-of-sight technique, such as e-beam (EB) evaporation [18, 19], but this type of deposition suffers from a non-uniform metal coverage. Unfortunately, other techniques which would not have this shortcoming, such as electrochemical plating [20], cannot be used due to the poor conductivity of the dielectric NWs. Hence, no matter how the NWs are oriented, randomly crossed or aligned and ordered, the challenge of fully coating them with a thin uniform layer of metal is still a serious issue.

Here, an approach based on a redox chemical reaction of silver plating is explored, which could potentially solve the problems related to incomplete metal coverage of the nanowires. It is known that the Tollens reaction is a silvering process often used to qualitatively detect the presence of aldehydes and reducing sugars, which also contain an aldehyde group [21]. Regardless of the reducing agent, the silver ion in the Tollens reagent can be reduced to neutral Ag which can be deposited on a substrate. In our experiments, we examine the effectiveness of the electroless (EL) plating technique by comparing the results of EL and e-beam (EB)

Ag deposition using random ZnO NWs grown on silicon. SERS investigation of both EL and EB silvered NWs were performed and compared. Furthermore, the topography, continuity and compositions of the EL and EB silver-sheathed NWs were characterized by scanning electron microscope (SEM) and energy dispersive x-ray (EDX) techniques. E-beam evaporation usually produced larger 2D islanded Ag films, while the electroless approach resulted in discrete and extremely closely spaced Ag nanoparticles, which were of the order of 20–30 nm in diameter. This should preclude the generation of a strong SERS enhancement, since the SPR of such particles would be weak in the UV [22], while our measurements were performed at 514.5 nm, which is significantly off the SPR peak. However, our results indicate a strong SERS signal from these small silver particle/nanowire composites. This surprising result is explained by our electric field simulations, which show that coupling effects between these small, closely spaced Ag islands and between the islands and the NW substrate can result in significant SERS enhancements. In addition, we show that the nanowire core, with its high density of facets, serves as a template for the nucleation of these closely space Ag islands, which allows the plasmonic coupling and hence the enhanced SERS signals.

2. Experimental details

The growth of the ZnO NWs was performed at 560 °C for 30 min in a horizontal furnace under atmospheric conditions, using an Si(100) substrate without a metal catalyst [17]. In this process, Zn powder was placed at the end of a quartz boat, and the substrates were placed at an appropriate distance from the source powder, generally no further than 1 inch.

The concentrated solutions for silver plating were from Peacock Lab and further diluted with deionized water. Specifically, four different solutions were involved in this silver plating process and their compositions as received are: (A) silver solution 'A': a mixture of 25–30 wt% silver diammine and 10–15 wt% ammonium hydroxide in water; (B) activator solution 'B': sodium hydroxide 10 wt% and ammonium hydroxide 5 wt% in water; (C) reducer solution 'C': 1 wt% formaldehyde in water and (D) sensitizer solution '#93': 20 wt% propyl alcohol, 5 wt% hydrochloric acid and 5 wt% stannous chloride in water. To meet the needs for the formation of the reproducible silver nanoparticles, we diluted all the received solutions by DI water. The dilution factors were 1:100 for solutions (A), (B) and (C), and 1:30 for solution (D) by volume. First, the substrate with the NWs was immersed in a dilute stannous chloride solution (D) for 15 s, and then the extra Sn^{2+} ions were removed by a deionized water rinse, keeping the surface wet. Thus, Sn^{2+} ions were absorbed on the surface of the ZnO NWs via electrostatic interaction, which could ensure the reproducibility in fully plating the dielectric nanowires. Next, the substrate was immersed in a mixture of equal amounts of the dilute silver solution (A), silver activator (B) and the reducer solutions (C) for 10–15 s. Finally the surface was fully rinsed with DI water and dried under flowing nitrogen.

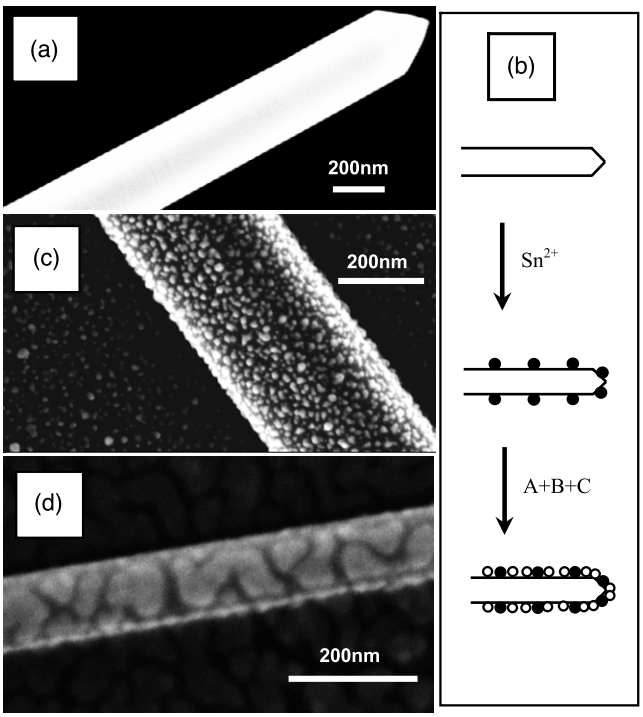

Figure 1. (a) SEM images of a bare nanowire as grown. (b) Schematic illustration of electroless (EL) silver plating on a single nanowire (A = silver ion solution, B = activator solution, C = reducer solution), (c) electroless (EL) Ag plated a single NW and (d) E-beam (EB) Ag evaporated a single NW.

7 nm silver depositions on ZnO NWs were performed by an FC-2000 Temescal E-beam metal evaporation system, at an evaporation rate of 1 Å s^{-1}.

The SERS measurements were carried out utilizing a confocal μ-Raman system which consisted of a Mitutoyo Microscope and an Ocean Optics QE65000 spectrometer equipped with a thermoelectrically cooled CCD. The 514.5 nm line of an Ar ion laser was used as the excitation source. The microscope utilized a 100 × 0.7 NA objective for focusing the laser light and was coupled to the spectrometer through a fiber optic cable. The spectra were collected with a low laser power of 0.75 mW at the sample. This was done to prevent desorption and damage to the benzene thiol and to prevent alterations to the Ag layer.

3. Results and discussion

As shown in figure 1(a), the lack of the catalyst on the tips of the ZnO NWs demonstrated that the growth process was a vapor–solid (VS) growth mode and catalyst-free. During the ZnO growth process, different NW shapes, including single, angled crossing and tetrapod shapes formed, and the NWs were randomly distributed on the silicon surface. The diameters varied from 50 to 300 nm and the length was of the order of several microns. Energy diffraction x-ray (EDX) analysis indicated that the chemical composition of the NWs was stoichiometric ZnO. Empirically the length and diameter of ZnO NWs depended on the growth time and gas flow rate. By controlling the growth conditions, very sparse distributions of

ZnO NWs on silicon were obtained, which were used in this study.

Figure 1(b) illustrates the sensitization and silver plating process. As described above, the concentrated solutions for electroless silver plating were further diluted with deionized water. During the silver plating process, the surface sensitizer [23, 24] Sn^{2+} ions and formaldehyde were respectively oxidized to Sn^{4+} and methanoic acid, while the Ag^{+} ions were reduced to neutral Ag and deposited on the ZnO NW surface uniformly. The chemical reactions can be roughly described as equation (1) below:

$$H_2CO(l) + 2[Ag(NH_3)_2][OH](aq) \rightarrow HCO_2H(aq) + 2Ag(s) + 4NH_3(aq) + H_2O(l). \quad (1)$$

Several different experimental conditions, including reaction temperature, solution concentration and reaction time, were used to optimize the silver plating process on the silicon substrate. The chemical reaction occurred very fast at room temperature when a high solution concentration was used. So, to form the uniform silver particles under this condition, it was hard to control the reaction process. Hence, we optimized the reaction conditions at room temperature by using diluted solutions and adjusting the reaction time. After numerous investigations, optimized conditions for the formation of homogeneous and reproducible particles were obtained: the substrate with the NWs was sensitized by diluted (1:30 v/v) solution (D) and then the silver plating process was carried out in a mixture of equal amounts of the diluted (1:100 v/v) solutions (A), (B) and (C) for 10–15 s at room temperature. The representative SEM image of silver plating is shown in figure 1(c), which displayed a uniform particle size and full coverage of the NWs. Shorter reaction times led to low silver coverage, and for longer reaction times, the existing particles coarsened and new particle nuclei also appeared, resulting in a rougher silver-covered surface, with a large particle size distribution. Similar EL silver coating results were observed for Ga_2O_3 NWs and vertically aligned ZnO NWs, using similar experimental conditions. This suggests that different surface energies of the two materials did not lead to significant changes in the EL nucleation process.

In contrast, another substrate with ZnO NWs was covered with 7 nm of silver via e-beam (EB) evaporation, which usually forms large discontinuous 2D islands, as shown in figure 1(d). The EDX analyses of both EL and EB Ag-covered ZnO NWs confirm the presence of Ag, which indicates the Ag was successfully deposited onto the nanowire surface. In comparison with the e-beam Ag-deposited NWs (figure 1(d)), the EL silver-plated ZnO NW surface (figure 1(c)) was uniformly covered with silver islands having an average diameter of 20–30 nm, spaced ≈10 nm apart, and displaying no particle aggregation or coarsening.

The advantage of EL silver plating over EB evaporation is that EB evaporation is a line-of-sight process, resulting in incomplete nanowire coverage. This is especially true for closely vertically aligned NWs or other oriented structures. To demonstrate this, both EL and EB silver-covered NWs were investigated by tilting the sample stage in the SEM investigations. As shown in figure 2, there is a clear shadow

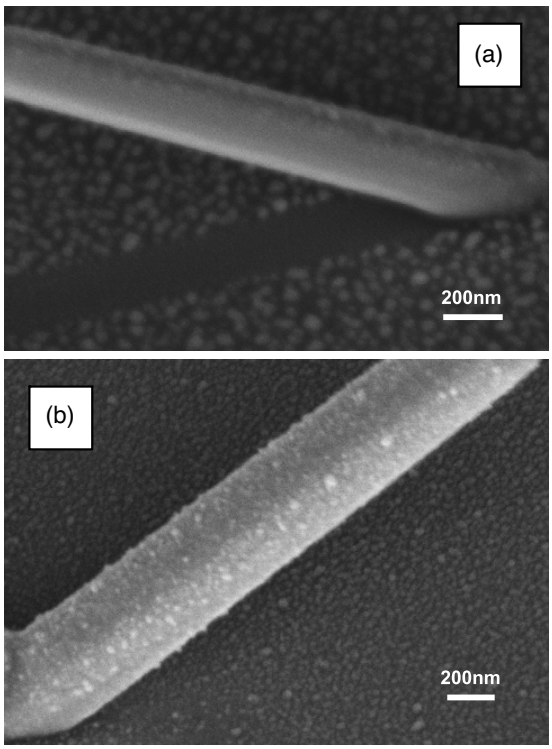

Figure 2. SEM images of e-beam (EB) deposited (a) and electroless (EL) plating (b) silver on ZnO NW, the angle between the incident electron beam and the sample stage is 45° for both (a) and (b).

area for the EB-deposited NW and the side of NW is lacking Ag coverage (figure 2(a)), while the EL-generated composites show no shadow regions and the sides of NWs are fully covered with Ag nanoparticles (figure 2(b)). This observation indicates that the NW surface can be fully covered with Ag by the EL plating approach. Furthermore, this approach is simple, fast and inexpensive, and allows the Ag coverage of gram quantities of nanowires at one time.

Figure 3(a) shows the representative SERS spectra measured on a single EL and EB-silvered NW. The major Raman peaks at 1002, 1071, 1386 and 1576 cm^{-1} can be assigned to symmetric ring breathing, in-plane C–H bending, wagging of the CH_2 groups and in-plane C–C stretching of the phenyl ring from benzene thiol, respectively [25–30]. As can be seen, the EL-silvered NWs result in a comparable SERS enhancement factor as that of the EB-silvered NWs. This is a surprising result since 20–30 nm silver nanospheres should not lead to a noticeable SERS signal enhancement for 514.5 nm excitation [8, 22]. This is because the SPR peak is in the UV part of the spectrum, as shown in figure 3(b). Note that, at 514.5 nm, one would expect an extremely weak enhancement since that is in the tail end of the calculated SPR. Since the EL-silvered NWs, shown in figure 1(c), are covered with small silver islands approximately 20–30 nm in diameter, spaced ≈10 nm apart, and they show a comparable SERS as the EB NWs suggests that there is a significant interaction between the spherical silver particles [31]. In addition, the particles also interact with the dielectric NW substrate, further increasing the enhancement. It should also be noted that Ag nanoparticles which deposit onto the Si substrate do not lead

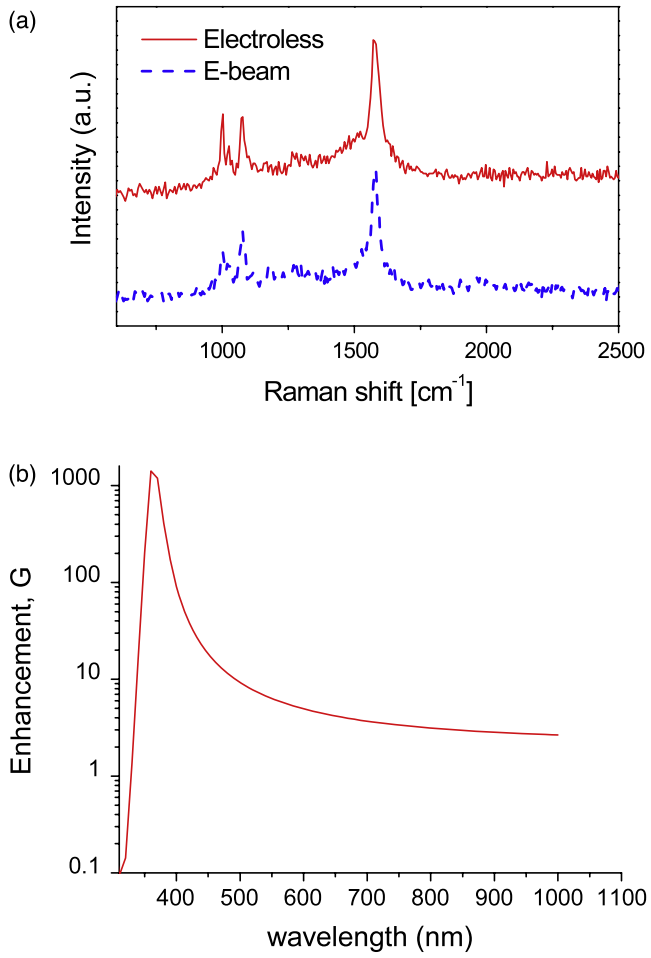

Figure 3. (a) Representative SERS on electroless (top solid curve) and E-beam (bottom dash curve) silver covered a single ZnO NW, and (b) surface plasmon resonance (SPR) simulation of 20 nm silver nanoparticles on ZnO NW.

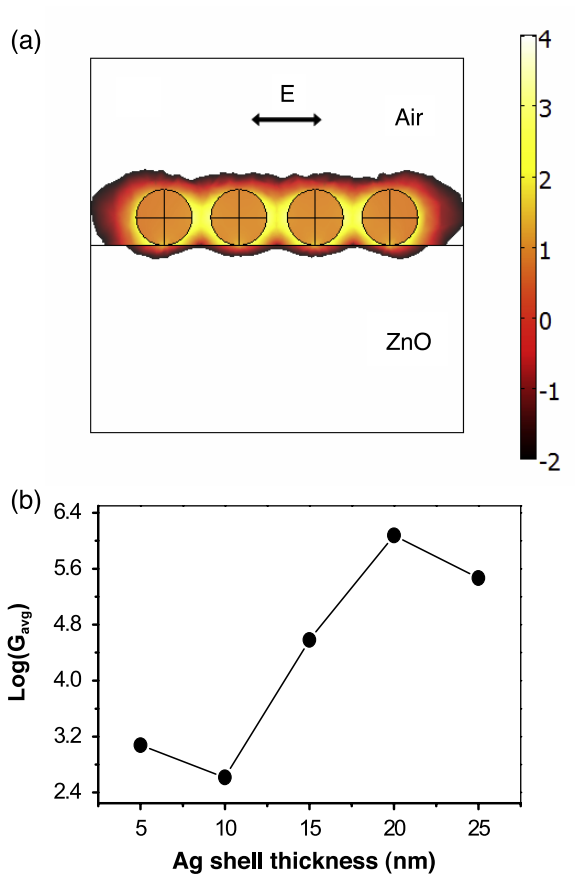

Figure 4. Simulations of log (G) for silver particles with the size of 30 nm on a ZnO substrate. (a) The direction of the electric field polarization is shown by the double arrow. (b) The Ag shell thickness dependence of the average SERS of a 60 nm diameter ZnO nanowire.

to any noticeable SERS, due to the fact that they are spaced further apart and thus no plasmon coupling occurs. This result also shows the importance of the dielectric nanowire as a substrate, since the dense Ag particle nucleation on these nanowires is most probably a result of a high density of microfacets, which are present on the nanowire surfaces [32] but which are absent on low index Si surfaces.

In order to better understand the SERS results, we performed a finite element 3D simulation of the enhancement for four closely spaced 30 nm diameter Ag shells on a ZnO substrate. The simulation was performed using the Comsol package and the quasistatic approximation, which is appropriate for object geometries and periodicities that are much smaller than the wavelength of light. Since the wavelength of light is 514.5 nm compared to 30 nm for the Ag spheres, the quasistatic approximation should provide good results.

Figure 4(a) shows a 3D simulation of the log of the enhancement, $G = (E/E_o)^4$, for four 30 nm Ag spheres spaced by 11 nm on a ZnO substrate. The wavelength of light is 514.5 nm. The calculations show that there is coupling between the spheres, which significantly increases the enhancement and moves it into the visible. In addition, we also see that the enhancement is about 10^3–10^4 in magnitude. In figure 4(b), we show the results of simulations as a function of Ag coating thickness for a uniformly coated ZnO nanowire that is 300 nm long and 60 nm in diameter. We see that below a shell thickness of 10 nm, the SERS enhancement of the nanowires is less than or equal to what one would expect from the closely spaced sphere of figure 4(a). This result explains why the enhancement of the EL-coated nanowires is similar to that of the EB-coated nanowires, even though the Ag coverage in the EL case is much higher. The EM coupling between the spherical EL particles spaced at distances comparable to half their radius and their interaction with the ZnO nanowire significantly increases their enhancement factor. The enhancement for this arrangement of nanoparticles on a dielectric surface is comparable to that of a uniformly coated ZnO nanowire with shell thicknesses of 10 nm or less.

To verify our simulation that the SERS signal is from the coupling of neighboring closely spaced nanoparticles, a control SERS measurement shown in figure 5 was performed on a single NW with sparse silver nanoparticles (the inset SEM image of figure 5). Due to the sparse and low coverage of silver nanoparticles on nanowires, no obvious SERS signal was observed which is in good agreement with our calculations. Note that the small feature around 970 cm^{-1} is from the silicon substrate.

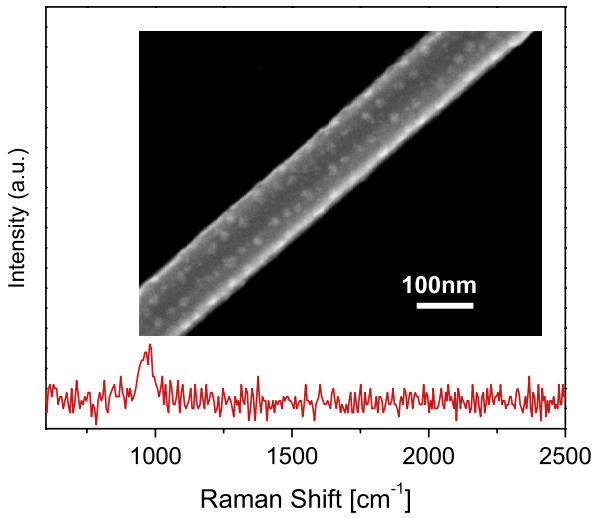

Figure 5. SERS measurement on a single nanowire with sparse silver nanoparticles, (inset) SEM image of a single nanowire with sparse silver nanoparticles produced via an electroless (EL) silver plating approach.

4. Summary

An easy, fast and reproducible electroless (EL) plating approach was employed to cover the NWs with silver, producing a sensitive dielectric NW core/metal sheath composite structure for SERS sensing. In comparison with the silver deposition via e-beam (EB) evaporation, this approach can result in the full metal coverage on NWs, regardless of the orientations and shapes of the nanostructures. SEM studies show that the NW surface was homogeneously fully covered with silver islands around 20–30 nm in diameter, spaced ≈10 nm apart. It is well demonstrated that NWs not only served as a necessary substrate for SERS enhancement, but also an indispensable template for the formation of extremely closely spaced and uniform silver nanoparticles. A strong SERS signal was surprisingly observed on the NWs covered with small silver 3D islands, although they are far below the size requirement for SERS generation. Our simulations indicate that the strong SERS signal from the NW composites covered with small silver islands is due to plasmonic coupling between the individual Ag islands on the curved NW surface, as well as coupling with the dielectric NW substrate. Control SERS experiment on a single NW with sparse silver nanoparticles, showing no SERS signal, confirmed the accuracy of the electric field simulations.

Acknowledgments

This work was partially supported by the Office of Naval Research (ONR). HQ thanks the American Society for Engineering Education (ASEE) program for administrative support. Dr Mazeina is thanked for helpful nanowire growth and discussion.

References

[1] Smythe E J, Dickey M D, Bao J, Whitesides G M and Capasso F 2009 *Nano Lett.* **9** 1132
[2] Xie J, Zhang Q, Lee J Y and Wang D I C 2008 *ACS Nano* **2** 2473
[3] Dickey M D, Weiss E A, Smythe E J, Chiechi R C, Capasso F and Whitesides G M 2008 *ACS Nano* **2** 800
[4] Yu Q, Guan P, Qin D, Golden G and Wallace P M 2008 *Nano Lett.* **8** 1923
[5] Schierhorn M, Lee S J, Boettcher S W, Stucky G D and Moskovits M 2006 *Adv. Mater.* **18** 2829
[6] Gunawidjaja R, Peleshanko S, Ko H and Tsukruk V V 2008 *Adv. Mater.* **20** 1544
[7] Hao E and Schatz G C 2004 *J. Chem. Phys.* **120** 357
[8] Nie S and Emory S R 1997 *Science* **275** 1102
[9] Kneipp K, Wang Y, Kneipp H, Perelman L T, Itzkan I, Dasari R R and Feld M S 1997 *Phys. Rev. Lett.* **78** 1667
[10] Dadosh T, Sperling J, Bryant G W, Breslow R, Shegai T, Dyshel M and Haran G 2009 *ACS Nano* **3** 1988
[11] Etchegoin P G, Ru E C L and Meyer M 2009 *J. Am. Chem. Soc.* **131** 2713
[12] Fleischmann M, Hendra P J and McQuillan A 1974 *J. Chem. Phys. Lett.* **26** 163
[13] Alvarez-Puebla R A, Contreras-Caceres R, Pastoriza-Santos I, Perez-Juste J and Liz-Marzan L M 2009 *Angew. Chem. Int. Edn* **48** 138
[14] Scholes F H, Bendavid A, Glenn F L, Critchley M, Davis T J and Sexton B A 2008 *J. Raman Spectrosc.* **39** 673
[15] Fang Y, Seong N and Dlott D D 2008 *Science* **321** 388
[16] Grand J, Chapelle M, Bijeon J L, Adam P M, Vial A and Royer P 2005 *Phys. Rev.* B **72** 033407
[17] Prokes S M, Glembocki O J, Rendell R W and Ancona M G 2007 *Appl. Phys. Lett.* **90** 093105
[18] Fang Y, Wei H, Hao F, Nordlander P and Xu H 2009 *Nano Lett.* **9** 2049
[19] Whitney A V, Van Duyne R P and Casadio F 2006 *J. Raman Spectrosc.* **37** 993
[20] D'Urzo L and Bozzini B 2009 *J. Mater. Sci., Mater. Electron.* **20** 217
[21] Beer J Z 1963 *J. Chromatogr.* **11** 247
[22] Emory S R, Haskins W E and Nie S 1998 *J. Am. Chem. Soc.* **120** 8009
[23] Kabayshi Y, Salgueirino-Maceira V and Liz-Marzan L M 2001 *Chem. Mater.* **13** 1630
[24] Schierhorn M and Liz-Marzan L M 2002 *Nano Lett.* **2** 13
[25] Jiang C, Lio W and Tsukruk V 2005 *Phys. Rev. Lett.* **95** 115503
[26] Ding J, Birss V and Liu G 1997 *Macromolecules* **30** 1442
[27] Sears W, Hunt J and Stevens 1981 *J. Chem. Phys.* **75** 1589
[28] Zucolotto V, Ferreira M, Cordeiro M, Constantino C, Balogh D, Zanatta A, Moreira W and Oliveira O 2003 *J. Phys. Chem.* B **107** 3733
[29] Aroca R and Thedchanamoorthy A 1995 *Chem. Mater.* **7** 69
[30] Kim J H, Kang T, Yoo S M, Lee S Y, Kim B and Choi Y K 2009 *Nanotechnology* **20** 235302
[31] Kottmann J P and Martin O J F 2001 *Opt. Express* **8** 655
[32] Mazeina L, Picard Y N and Prokes S M 2009 *Cryst. Growth Des.* **9** 1164